Hierarchical model predictive control of Venlo-type greenhouse climate for improving energy efficiency and reducing operating cost

Dong Lin [*], Lijun Zhang [*], Xiaohua Xia

Department of Electrical, Electronic and Computer Engineering, University of Pretoria, Pretoria, 0002, South Africa

ARTICLE INFO

ABSTRACT

In this paper, a hierarchical control strategy for Venlo-type greenhouse climate control under South Africa climate is proposed to improve energy efficiency and reduce operating cost. The proposed hierarchical control architecture includes two layers. The upper layer is to generate set points by solving different optimization problems. Three different strategies with different optimization objectives are studied. The meteorological data of a typical winter day is used. Strategy 1 is to minimize the energy consumption. Strategy 2 is to minimize the energy cost under the time-of-use (TOU) tariff. Strategy 3 is to minimize the total cost of energy consumption, ventilation and carbon dioxide (CO_2) supply. The lower layer is to track the trajectories obtained from the upper layer. A closed-loop model predictive control (MPC) strategy is introduced to address model plant mismatch and reject system disturbances. Two performance indices, relative average deviation (RAD) and maximum relative deviation (MRD), are introduced to compare the tracking performance of the proposed MPC and an open loop control under three different levels of system disturbances (2%, 5%, 10%). Simulation results show that the proposed strategy can effectively reduce the operating cost while keeping the temperature, relative humidity and CO_2 concentration within required ranges. Compared with Strategy 1 and Strategy 2, the total cost of Strategy 3 is reduced by 72.07% and 71.41% respectively. Moreover, the proposed MPC has better tracking performance than the open loop control. Therefore, the proposed hierarchical MPC strategy could be an effective way to improve greenhouse energy efficiency and achieve sustainable cleaner production.

© 2020 Elsevier Ltd. All rights reserved.

1. Introduction

With the increase of population and the decrease of cultivable lands, the problem of food shortage is becoming more and more serious in some countries (Hassanien et al., 2016; Yano and Cossu, 2019). In addition, in some arid regions, freshwater demand is increasingly difficult to meet (Liu et al., 2020, 2019). Greenhouse cultivation is an effective way to solve these problems. Crops grown in the greenhouse can get higher yields than that grown outdoor (Esen and Yuksel, 2013). Moreover, greenhouse cultivation consumes less water than outdoor planting mode (Garg and Dadhich, 2014). Therefore, the research on agricultural greenhouse can help to solve the problem of food shortage and effectively alleviate the current water crisis.

A Venlo–type greenhouse is a commonly used greenhouse in agricultural production. Farmers can adjust the greenhouse climate according to their preferences with controllers, to keep the temperature, humidity, CO_2 concentration, and light intensity within desired ranges (Van Henten, 1994; Yang and Rhee, 2013). However, due to the problems of operation strategy, some greenhouses have low energy efficiency and high production cost.

The greenhouse climate control process consumes lots of energy to keep greenhouse climatic conditions within required ranges (Fox et al., 2019). The main energy sources include electricity energy, coal, fuel oil, natural gas, and clean energy such as wind energy and solar energy (Vadiee and Martin, 2014; Cuce et al., 2016). Coal and fuel oil can be used as backup energy to power greenhouses during power outages. The high energy consumption will increase both greenhouse production cost and greenhouse gas emissions (Van Henten and Bontsema, 2009). For example, in the United States, greenhouse energy consumption accounts for 16% of agricultural energy consumption (Bozchalui et al., 2014). In some cases, energy costs account for 50% of the total cost of greenhouse production (Shen et al., 2018). Some approaches have been proposed to solve

this problem. For instance, a fuzzy control strategy for greenhouse climate to minimize production cost is proposed in (Lafont and Balmat, 2002). A robust control method is proposed in (Bennis et al., 2008). A PID controller for greenhouse climate system is designed in (Hu et al., 2011). An adaptive fuzzy control strategy is studied in (Su et al., 2016). Under these control strategies, the greenhouse climatic factors such as temperature and humidity can be kept within required ranges. However, energy efficiency is still low due to the lack of energy optimization processes.

Some control strategies considered energy optimization. For instance, a control method to reduce the energy consumption of greenhouse heating is proposed in (Chen et al., 2015). In (Ramírez-Arias et al., 2012), a multi-objective control strategy for greenhouse crop growth is proposed to maximize profit, fruit quality and water-use efficiency. In (Blasco et al., 2007), a model-based predictive control strategy is proposed to reduce the energy and water consumption of the greenhouse. However, these studies only considered the cost of energy consumed for greenhouse control. The cost of ventilation and CO_2 supply, which accounts for a large part of production costs, is ignored. Moreover, the time-of-use (TOU) tariff was not considered in these studies.

Greenhouse modelling is also challenging because of the complexity of the greenhouse environment. For example, the controlled variables (temperature and humidity) are correlated and sensitive to the outside weather (Chen et al., 2016; Du et al., 2012). In addition, the growth of crops has a strong impact on climate change inside the greenhouse (Rodríguez et al., 2008). For example, the transpiration of crops can affect greenhouse humidity (Su et al., 2017). Therefore, it is difficult to accurately model the dynamic process of greenhouse climate.

In the field of greenhouse climate modelling, there are different methods in the literature. In (Ferreira et al., 2002; Frausto and Pieters, 2004), a black box model is presented by analyzing the input and output data of the greenhouse system. However, this modelling method generally requires lots of data to ensure the accuracy of the model. Moreover, the model built may not be suitable for greenhouses with different configurations (Tap, 2000). Some modelling processes are based on first principles by analyzing the physical, chemical and biological laws involved in the process. For example, a dynamic model based on energy and mass balances is proposed in (Van Beveren et al., 2015a, b). This modelling method gives a detailed description of the climate control process. Both the effects of crop transpiration and the interference of external conditions are taken into consideration. The experimental results show that the proposed model has a good performance regarding greenhouse climate control.

The accuracy of traditional control strategies is low due to system disturbances and model uncertainties. The climatic conditions outside the greenhouse such as temperature, humidity, solar radiation, wind speed have a great impact on the climate in the greenhouse (Chen et al., 2018). In order to solve this problem, different control methods are proposed. A robust control strategy for greenhouse temperature and CO_2 concentration control is proposed in (Linker et al., 1999). An adaptive fuzzy control strategy is presented in (Su et al., 2015). Some research studied the application of model predictive control (MPC) for greenhouse climate control, such as (Coelho et al., 2005; Gruber et al., 2011). The greenhouse control system can react before any deviation of the controlled variables occurs, thus avoiding the response delay. However, the proposed MPC is only used for greenhouse temperature control, not for humidity and CO_2 concentration control.

MPC uses the model of the plant to predict the future response over a finite horizon. A control sequence is obtained by solving an optimization problem online. Only the first value of the response sequence is applied to the next sampling interval, the rest values

are discarded (Wu et al., 2015; Zhu et al., 2014). Due to the closed-loop nature of MPC, it can effectively address system disturbances and is widely used in process control such as urban household water management (Wanjiru et al., 2016), industrial fermentation process control (Mohd and Aziz, 2016), building performance optimization (Cao et al., 2019), heavy-haul train control (Zhang and Zhuan, 2013, 2015) and air conditioning system optimization (Mei and Xia, 2017; Sayadi et al., 2019).

In South Africa, the food shortage problem is serious. About 35% of South Africa's population does not have access to adequate food (Erna du Plessis et al., 2015). One reason is that many lands are not suitable for traditional outdoor planting. Crop yields are vulnerable to climate change. Moreover, the energy shortage problem is also very serious in South Africa (Menyah and Wolde-Rufael, 2010; Kohler, 2014). In 2019, a stage 4 load shedding was implemented to prevent the collapse of the power system, which has a negative impact on people's lives.

In this paper, the climate control of a Venlo-type greenhouse under South Africa climate is studied. The main objective of this paper is to analyze different control strategies for a typical modern greenhouse system to improve energy efficiency and reduce production cost. The dynamic model presented in (Van Beveren et al., 2015a, b) is adopted. A hierarchical control strategy is proposed. The proposed hierarchical control architecture is divided into two layers. On the upper layer, three different strategies with different optimization objectives are proposed to find the optimal operation trajectories. Strategy 1 is to minimize the energy consumption for greenhouse heating and cooling. Strategy 2 is to minimize the energy cost under the TOU tariff. Strategy 3 is to minimize the total cost which includes energy cost, ventilation cost and CO_2 supply cost. On the lower layer, a model predictive controller is designed to track the trajectories obtained from the upper layer.

The main contributions of this paper are as follows: (1) A hierarchical control architecture for greenhouse climate control is adopted. The proposed hierarchical control strategy can effectively reduce the computational complexity of optimization problems. (2) Three different optimal strategies are studied to reduce greenhouse cost. Not only energy cost but also ventilation and CO_2 supply cost are taken into consideration for the optimization of operating cost. Compared with traditional control methods, the proposed control strategy can greatly reduce greenhouse operating costs. (3) An MPC strategy is used to reduce the influence of system disturbance and model plant mismatch. The system control accuracy is improved.

The rest of this paper is organized as follows: System description is presented in Section 2. The hierarchical control strategy is described in Section 3. The climate controller design is conducted in Section 4. The simulation results are discussed in Section 5. Section 6 is the conclusion.

2. System description

A greenhouse is a building structure with walls and roofs that are made of transparent materials such as glasses and plastics. The cover prevents energy loss and keeps the indoor temperature higher than that of the outside. The ventilation reduces humidity in greenhouses and provides CO_2 for crops. The sunlight provides the light crops need. However, sometimes the greenhouse climate cannot be maintained within the required range. For instance, when the outdoor temperature is too low, additional heating is needed. Moreover, in order to obtain higher yield and better quality, extra CO_2 and lighting should be supplied. Therefore, a greenhouse climate control system is essential to keep the internal climate within suitable ranges.

The structure of the greenhouse climate control system is shown in Fig. 1. These systems can be controlled by growers, or can
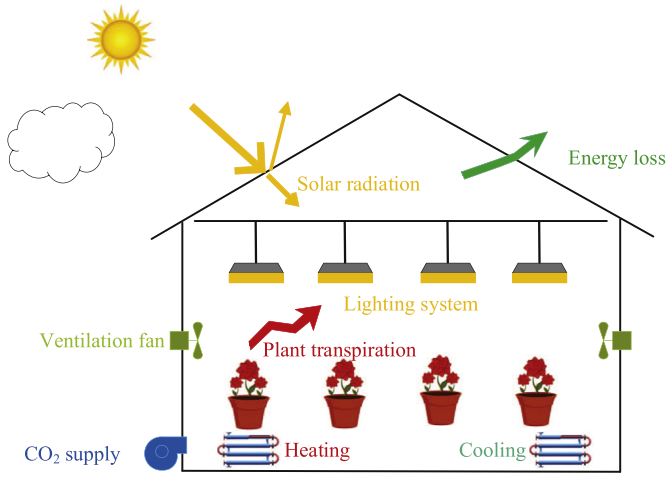
Fig. 1. Greenhouse climate control system structure.

automatically respond to external conditions and manipulate internal climate accordingly. Fig. 2 is the schematic diagram of the greenhouse control process. Firstly, farmers set control objectives and system constraints according to their experience. Then, the controller calculates the optimal control variables based on the electricity price, climate data in the greenhouse, and outdoor weather data. Finally, actuators regulate the greenhouse climate according to the control signal obtained from the controller.

2.1. Greenhouse climate model

Greenhouse climate control is a multi-input multi-output (MIMO) system. Greenhouse climate control generally includes temperature control, relative humidity control, CO_2 concentration control and lighting control. In this paper, the greenhouse climate control system studied includes three inputs (heating, ventilation and CO_2 injection) and three outputs (temperature, relative humidity and CO_2 concentration).

The dynamic model about temperature, humidity and CO_2 concentration control presented in (Van Beveren et al., 2015a, b) is adopted, and briefly introduced in the following. Please note that
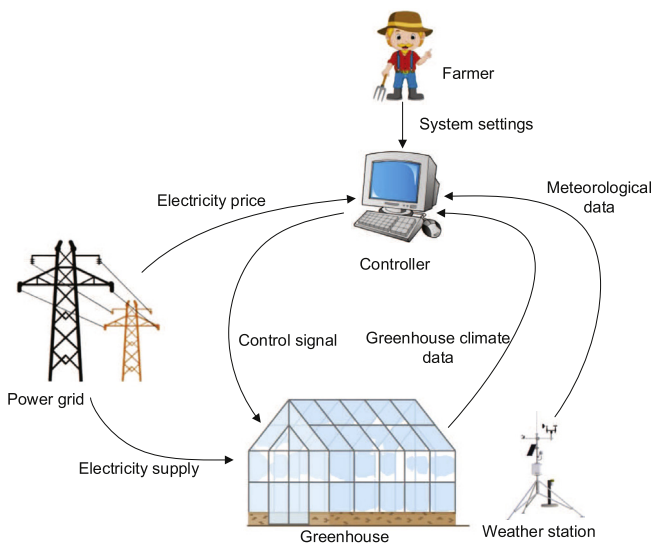

Fig. 2. Schematic diagram of greenhouse control process.

the model is based on the energy and mass balances of the greenhouse per unit area.

2.1.1. Temperature model

Greenhouse temperature modeling is based on the energy balance of the greenhouse. The temperature is governed by:

$$\frac{dT_{air}}{dt} = \frac{1}{C_{cap}} \left(Q_{sun} + Q_{lamp} - Q_{cov} - Q_{trans} - Q_{vent} + Q_c \right), \tag{1}$$

where T_{air} is the temperature inside the greenhouse, C_{cap} is the heat capacity of the greenhouse, Q_{sun} is the incoming radiation from the sun, Q_{lamp} is the lamp heating power. Q_{cov} is the heat transfer through the cover, Q_{trans} is the energy absorption of crop transpiration. Q_{vent} is the energy exchange through ventilation. Q_c is the heating or cooling power. All variables used in this paper are defined in the nomenclature shown in Table 1.

Q_{sun} can be calculated by:

$$Q_{sun} = \alpha_1 I_{rad}, \tag{2}$$

where α_1 is the transmission coefficient of the cover material and I_{rad} is the solar radiation power.

Q_{cov} can be described by:

$$Q_{cov} = \alpha_2 (T_{air} - T_{out}), \tag{3}$$

where α_2 is the heat transfer coefficient of the cover, T_{out} is the outside temperature.

Q_{trans} can be obtained by:

$$Q_{trans} = g_e L (H_{crop} - H_{air}), \tag{4}$$

where g_e is the transpiration conductance, L is the amount of energy needed to evaporate water from a leaf. H_{crop} is the absolute water vapour concentration at crop level. H_{air} is the absolute water vapour concentration of the greenhouse air.

H_{crop} can be calculated by:

$$H_{crop} = H_{air,sat} + \varepsilon \frac{r_b}{2LAI} \frac{R_n}{L}, \tag{5}$$

where $H_{air,sat}$ is the saturated vapour concentration. According to (Bontsema et al., 2008), $H_{air,sat}$ can be approximated by:

$$H_{air,sat} = 5.5638 e^{0.0572 T_{air}}. \tag{6}$$

g_e is obtained using:

$$g_e = \frac{2LAI}{(1 + \varepsilon) r_b + r_s}, \tag{7}$$

where LAI is the leaf area index, ε is the ratio of latent to sensible heat content of saturated air. r_b is the boundary layer resistance, r_s is the stomatal resistance.

ε and r_s can be obtained by:

$$\varepsilon = 0.7584 e^{0.0518 T_{air}}, \tag{8}$$

$$r_s = \left(82 + 570 e^{-\gamma \frac{R_n}{LAI}} \right) \left(1 + 0.023 (T_{air} - 20)^2 \right), \tag{9}$$

where γ is a crop specific parameter, R_n is the net radiation at crop level and given by:

Table 1
Nomenclature.

T_{air}	air temperature in the greenhouse, °C
RH_{air}	relative humidity in the greenhouse, %
T_{out}	air temperature outside the greenhouse, °C
I_{rad}	solar radiation power, W/m^2
Q_{sun}	incoming radiation power, W/m^2
α_1	transmission coefficient
Q_{lamp}	lamp heating power, W/m^2
α_2	heat transfer coefficient, W/°Cm2
Q_{cov}	heat transfer through the cover, W/m^2
g_e	transpiration conductance, m/s
Q_{trans}	transpiration endothermic power, W/m^2
L	energy needed to evaporate water from a leaf, J/g
Q_{vent}	heat loss through ventilation power, W/m^2
Q_c	controlled heating or cooling power, W/m^2
LAI	leaf area index
H_{air}	humidity in the greenhouse, g/m^3
ε	ratio of latent to sensible heat content of saturated air
H_{trans}	vapour evaporated by the crop, g/m^{2}s
H_{cov}	vapour condensation to the cover, g/m^{2}s
r_b	boundary layer resistance parameter, s/m
H_{crop}	vapour concentration at crop level, g/m^3
r_s	stomatal resistance, s/m
H_{out}	humidity outside the greenhouse, g/m^3
γ	crop specific parameter
H_{vent}	vapour flux due to ventilation, g/m^{2}s
P_E	artificial lighting power, W/m^2
RH_{air}	relative humidity in the greenhouse, %
η	lighting thermal conversion coefficient
C_{air}	CO$_2$ concentration in the greenhouse, g/m^3
g_v	ventilation rate, m/s
C_{out}	CO$_2$ concentration outside the greenhouse, g/m^3
s	the greenhouse area, m^2
C_{inj}	CO$_2$ injection into the greenhouse, g/m^{2}s
ρ_{air}	density of air, kg/m^3
C_{ass}	CO$_2$ assimilation by the crop, g/m^{2}s
h	average height of greenhouse, m
C_{vent}	effect of ventilation on CO$_2$ concentration, g/m^{2}s
g_c	the condensation conductance, m/s
C_{cap}	heat capacity of the greenhouse, J/°Cm^2
p_{gc}	parameter related to the properties of the condensation surface, m°C$^{-\frac{1}{3}}$s^{-1}
$C_{p,air}$	heat capacity of the air, J/kg°C

$$R_n = 0.86\left(1 - e^{-0.7LAI}\right)\left(Q_{sun} + P_E\right), \tag{10}$$

where P_E is the rated electric power of artificial lighting installed.

$$Q_{lamp} = \eta P_E, \tag{11}$$

where η is the part of electric energy consumption of the lamps that is converted into heat.

$$Q_{vent} = g_v \rho_{air} C_{p,air}(T_{air} - T_{out}), \tag{12}$$

where g_v denotes the specific ventilation rate, ρ_{air} is the density of the air, $C_{p,air}$ is the specific heat capacity of the air.

2.1.2. Relative humidity model

The factors affecting the change of greenhouse relative humidity include crop transpiration, vapour condensation, and ventilation. The relative humidity RH_{air} can be obtained using:

$$RH_{air} = H_{air}/H_{air,sat}, \tag{13}$$

where H_{air} is the vapour concentration of the greenhouse air. H_{air} can be calculated by:

$$\frac{dH_{air}}{dt} = \frac{1}{h}(H_{trans} - H_{cov} - H_{vent}), \tag{14}$$

where H_{trans} is the vapour produced by plant transpiration, H_{cov} is the vapour condensation to the cover, H_{vent} is the vapour flux due to ventilation. h is the average height of greenhouse.

H_{trans} is influenced by H_{crop} and H_{air}, and it can be described by:

$$H_{trans} = g_e\left(H_{crop} - H_{air}\right). \tag{15}$$

H_{cov} can be modelled by the following equation:

$$H_{cov} = g_c\left[0.2522e^{0.0485T_{air}}(T_{air} - T_{out}) - (H_{air,sat} - H_{air})\right], \tag{16}$$

where g_c is the condensation conductance, and it can be calculated by:

$$g_c = \begin{cases} 0 & \text{if} \quad T_{air} \leq T_{out}, \\ p_{gc}(T_{air} - T_{cov})^{1/3} & \text{if} \quad T_{air} > T_{out} \end{cases} \tag{17}$$

where p_{gc} is related to the properties of the condensation surface.

H_{vent} is influenced by the ventilation and the humidity both inside and outside greenhouse. The value of H_{vent} can be obtained by:

$$H_{vent} = g_v(H_{air} - H_{out}), \tag{18}$$

where g_v is the ventilation rate and controlled by the power of fans.

2.1.3. CO_2 concentration Model

The CO_2 concentration model based on mass balance is as follows.

$$\frac{dC_{air}}{dt} = \frac{1}{h}(C_{inj} - C_{ass} - C_{vent}), \tag{19}$$

where C_{air} is the CO_2 concentration inside the greenhouse, C_{inj} is the CO_2 injection rate, C_{ass} is the CO_2 assimilation, C_{vent} is the changes in CO_2 concentration due to ventilation.

C_{ass} and C_{vent} can be obtained by:

$$C_{ass} = 2.2 \times 10^{-3} \frac{1}{1 + \frac{0.42}{C_{air}}} \left(1 - e^{-0.003(Q_{sun} + P_E)}\right), \tag{20}$$

$$C_{vent} = g_v(C_{air} - C_{out}). \tag{21}$$

2.1.4. Model performance analysis

The models proposed had been validated in (Van Beveren et al., 2015a, b). Two performance indices, correlation coefficient (r) and root mean square error (RMSE), are calculated to analyze the model performance. The greenhouse climate data of one whole year is used for the model performance analysis. The results show that the predicted values can follow the actual values well in most cases. In some cases, there is a big difference between the predicted value and the actual measured value such as in February when the outside temperature is very low. Similar results can be found in (Su et al., 2018). The average winter temperature in South Africa is much higher than that in the Netherlands. For example, in Pretoria, the administration capital of South Africa, the average temperature of the winter is also above 10°C. Therefore, the proposed model in (Van Beveren et al., 2015a, b) can be used for greenhouse control in South Africa.

2.2. System constraints

2.2.1. State constraints

Too high or too low temperature, relative humidity and CO_2 concentration will have a negative impact on both crops yields and quality (Kläring et al., 2007). For instance, too high relative humidity in the greenhouse will accelerate the spread of pests and diseases, too high or too low temperature will result in crop wilting and even death. Therefore, the state variables should be kept within appropriate ranges to provide suitable growing conditions for crops. Moreover, for different type of crops, the ranges are different. The ranges are determined by farmers' experience or the results obtained from the optimization of crop growth control process. The state constraints are represented by the following.

$$T_{air,min} \leq T_{air} \leq T_{air,max}, \tag{22}$$

$$RH_{air,min} \leq RH_{air} \leq RH_{air,max}, \tag{23}$$

$$C_{air,min} \leq C_{air} \leq C_{air,max}, \tag{24}$$

where $T_{air,min}$ and $T_{air,max}$ are the lower and upper bounds of temperature, $RH_{air,min}$ and $RH_{air,max}$ are the lower and upper bounds of relative humidity, and $C_{air,min}$ and $C_{air,max}$ are the lower and upper bounds of CO_2 concentration.

2.2.2. Input constraints

There are also some input constraints, such as the operational constraints and physical limits below.

$$Q_{c,min} \leq Q_c \leq Q_{c,max}, \tag{25}$$

$$g_{v,min} \leq g_v \leq g_{v,max}, \tag{26}$$

$$C_{inj,min} \leq C_{inj} \leq C_{inj,max}, \tag{27}$$

where $Q_{c,min}$ and $Q_{c,max}$ are the lower and upper bounds of heating or cooling power. $g_{v,min}$ and $g_{v,max}$ are the lower and upper bounds of ventilation rate. $C_{inj,min}$ and $C_{inj,max}$ are the lower and upper bounds of CO_2 injection rate.

To reduce the wear of actuators, extreme changes should be prevented (Durand et al., 2016). Therefore, the following input rate of change constraints are adopted:

$$\left|\frac{dQ_c}{dt}\right| \leq k_1, \tag{28}$$

$$\left|\frac{dg_v}{dt}\right| \leq k_2, \tag{29}$$

$$\left|\frac{dC_{inj}}{dt}\right| \leq k_3, \tag{30}$$

where k_1, k_2 and k_3 are the change rate limits of input variables Q_c, g_v and C_{inj} respectively.

3. Hierarchical control strategy

The hierarchical control can effectively reduce the computational complexity of complex problems by decomposing them into different subproblems, which is widely used in building energy optimization processes (Mei et al., 2018). The hierarchical control architecture of greenhouse climate is shown in Fig. 3. On the upper layer, an optimization problem that takes into account weather data and energy price is solved to obtain the set points. On the lower layer, a climate controller is designed to track the reference trajectories obtained from the upper layer.

3.1. Upper layer (optimization layer)

The upper layer is to find the set points for greenhouse climate controllers. In this paper, three different strategies with different optimization objectives are studied. For these optimization problems, the control variables are the heating or cooling power Q_c, ventilation rate g_v and CO_2 injection rate C_{inj}. The controlled variables are the temperature T_{air}, relative humidity RH_{air} and CO_2 concentration C_{air}.

The objective of Strategy 1 is to minimize the energy consumption for greenhouse heating and cooling. Therefore, the optimization objective of Strategy 1 can be given by:

$$J_1 = \int_{t_i}^{t_f} |Q_c(t)| dt, \tag{31}$$

where t_i is the initial time, t_f is the final time of optimization.

The objective of Strategy 2 is to minimize the energy cost under
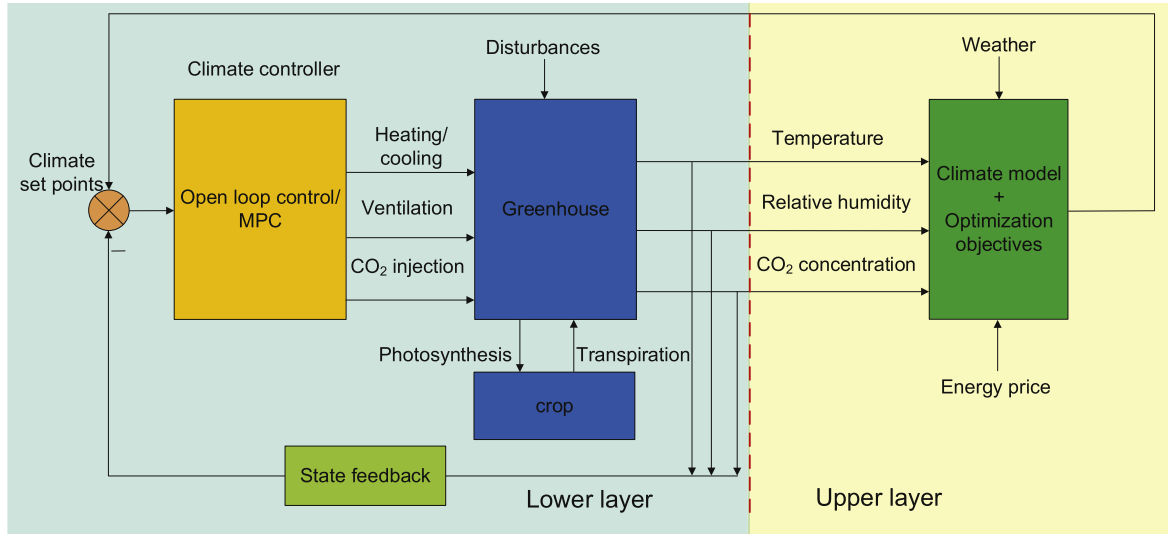
Fig. 3. Greenhouse climate hierarchical control architecture.

the TOU tariff. The objective function of Strategy 2 is as follows.

$$J_2 = \int_{t_i}^{t_f} |Q_c(t)w(t)| dt, \tag{32}$$

where $w(t)$ is the electricity price at the time t. In this study, the TOU tariff in South Africa is used and given by:

$$w(t) = \begin{cases} w_o & t \in [0,6] \cup [22,24] \\ w_s & t \in [9,17] \cup [19,22], \\ w_p & t \in [6,9] \cup [17,19] \end{cases} \tag{33}$$

where w_o, w_s, w_p are the off-peak, standard, peak tariff in R/ kWh. R is the South Africa Currency, Rand. The value of w_o, w_s, w_p are 0.5157, 0.9446, 3.1047 respectively.

The objective of Strategy 3 is to minimize the total operating cost which includes the energy cost, ventilation cost and CO_2 supply cost. The energy cost can be obtained from (32). The ventilation cost is the cost of electricity consumed by the ventilation fan. In this paper, the on-off control method is adopted for ventilation fan operation. The CO_2 cost is determined by the amount of the CO_2 consumed and the price of the CO_2. The objective function of Strategy 3 can be obtained by:

$$J_3 = \int_{t_i}^{t_f} (Q_c(t)w(t) + g_v(t)\lambda w(t) + C_{inj}(t)p_c) dt, \tag{34}$$

where p_c is the price of organic CO_2. $p_c = $ R1000/ton. λ is the conversion coefficient from the ventilation rate (g_v) to the ventilation fan power (Q_v). $\lambda = 0.06$ W/m^3.

The optimization problem (31), (32) and (34) are subject to the constraints from (22) to (30).

3.2. Lower layer (control layer)

The lower layer to track the reference trajectories obtained from the upper layer. In this paper, a closed-loop model predictive controller is designed and compared with the open loop controller. Two performance indices (relative average deviation and maximum relative deviation) are introduced to compare the

tracking performance of the proposed model predictive control and an open loop control under different levels of system disturbances.

4. Climate controller design

4.1. Open loop control

The continuous state-space model is as follows:

$$\dot{x} = f(x, u). \tag{35}$$

In order to facilitate the controller, (35) is discretized to:

$$x(k+1) = f(x(k), u(k)), \tag{36}$$

where k is the current time kT_s, T_s is the sampling interval. $x(k) = [T(k), RH(k), C(k)]^T$, $T(k)$, $RH(k)$ and $C(k)$ are the temperature, humidity and CO_2 concentration at time k respectively. The objective function that derives from (34) is adopted and given by:

$$J_o = \sum_{k=1}^{N} |Pu(k)|, \tag{37}$$

where $N = \frac{T}{T_s}$. T is the total simulation time. $u(k) = [u_1(k), u_2(k), u_3(k)]^T$, $u(k)$ is the input variables at the time $k = 1, 2, 3, \cdots, N$. u_1, u_2 and u_3 are the heating/cooling power (Q_c), ventilation rate (g_v) and CO_2 injection rate (C_{inj}), respectively. For Strategy 1, $P = [1, 0, 0]$. For Strategy 2, $P = [w, 0, 0]$. For Strategy 3, $P = [w, \lambda w, p_c]$.

The open loop controller solves the optimization problem:

$$u_{ref}^* = \underset{u}{\arg\min} J_o, \tag{38}$$

subject to the constraints $(22) - (30)$ and (36).

4.2. Closed-loop MPC

For closed-loop MPC, the input variables obtained from (38) are taken as the inputs reference trajectories u_{ref}, and the corresponding state variables are taken as the state variables reference trajectories x_{ref}. The objective function is as follows:

$$J_m = \sum_{i=1}^{N_p} (\Delta x(k+i|k))^T Q(\Delta x(k+i|k))$$
$$+ \sum_{i=1}^{N_c} (\Delta u(k+i-1|k))^T R(\Delta u(k+i-1|k)), \quad (39)$$

where N_p and N_c are optimization horizon and control horizon respectively. Q and R are the weighting matrices. $|k$ means that the predicted value is based on the information up to time k. $\Delta x(k+i|k)$ is the changes of state variables because of Δu. Δu is the change of input variables, and it is used to compensate model plant mismatch and system disturbances. $\Delta x(k+i|k)$ and Δu are given by

$$\Delta x(k+i|k) = x(k+i|k) - x_{ref}(k+i), \quad (40)$$

$$\Delta u(k) = u(k|k) - u_{ref}(k). \quad (41)$$

Denote $\Delta U = [\Delta u(k|k), \Delta u(k+1|k), \Delta u(k+2|k), \cdots, \Delta u(k+N_c-1|k)]^T$. The MPC controller solves the nonlinear optimization problem

$$\Delta U^*(k) = \underset{\Delta U}{\arg\min} J_m(k), \quad (42)$$

subject to the constraints $(22) - (30)$ and (36). The optimal control is implemented in a receding horizon scheme that the first value of $\Delta U^*(k)$ is adopted and the rest are discarded.

$$\Delta u(k) = \Delta u^*(k|k), \quad (43)$$

where $\Delta u^*(k|k)$ is the first entry of $\Delta U^*(k)$. Repeat the above steps until k reaches the predefined value. The final optimal inputs obtained by the MPC controller is given by: $u(k) = u_{ref}(k) + \Delta u(k)$.

5. Simulation

5.1. Simulation parameters

In this paper, a Venlo-type greenhouse is studied. The parameters of the greenhouse model are derived from (Van Beveren et al., 2015a, b) and listed in Table 2.

The greenhouse area s is 40709 m^2 and the average height is 7 m. There are 4536 SON-T lamps installed for providing artificial lighting. For each 80 m^2, one air-to-water heat exchanger is installed for heating and cooling. Fans and windows are used for ventilation.

An OCAP (organic CO_2 for assimilation by plants) network is used to supply organic CO_2. The price of CO_2 delivered by OCAP pipeline is R 1000 per ton. An axial plate type fan is used for ventilation. The power of each fan is 300 W. The air flow is 5000 m^3 per hour. There are eight HortiMaX® measurement boxes for climate data measurement. To achieve a uniform greenhouse climate state, the measurement boxes and greenhouse climate control actuators are uniformly distributed.

The meteorological data such as solar radiation, outdoor temperature and outdoor relative humidity are from a weather station at the University of Pretoria. The data for a typical winter day (July 13, 2016) is used and shown in Fig. 4 and Fig. 5. Please note that the light power is not a control variable. For day time (07:00 to 18:00), the lighting power is set to zero. For night time (19:00 to 06:00), the lighting power is set to 110 W/m^2. The outdoor CO_2 concentration is 407 ppm. The initial value needs to be within a reasonable range of the greenhouse climate. In this paper, the initial value selected

Table 2
Parameters of the greenhouse model.

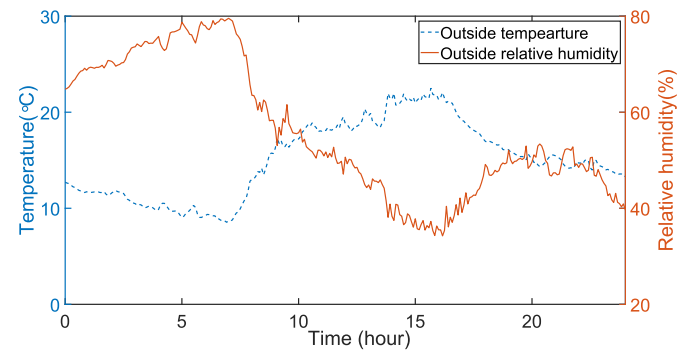| Variable	Value	Unit
α_1	0.7	–
α_2	10	–
γ	0.008	–
LAI	2.6	–
C_{cap}	30000	J/m^2 °C
h	7	m
s	40709	m^2
L	2450	J/g
r_b	150	s/m
ρ_{air}	1.225	kg/m^3
$C_{p,air}$	1003	J/kg°C
p_{gc}	1.8×10^{-3}	m°C$^{-1/3}$s^{-1}
$T_{air,min}$	14	°C
$T_{air,max}$	26	°C
$RH_{air,min}$	0	%
$RH_{air,max}$	90	%
$C_{air,min}$	400	ppm
$C_{air,max}$	2000	ppm
$Q_{c,min}$	−200	W/m^2
$Q_{c,max}$	200	W/m^2
$g_{v,min}$	0	m/s
$g_{v,max}$	0.05	m/s
$C_{inj,min}$	0	g/m^{2}s
$C_{inj,max}$	0.05	g/m^{2}s
k_1	0.51	W/m^{2}s
k_2	5.1×10^{-5}	m/s^2
k_3	5.1×10^{-5}	g/m^{2}s^2

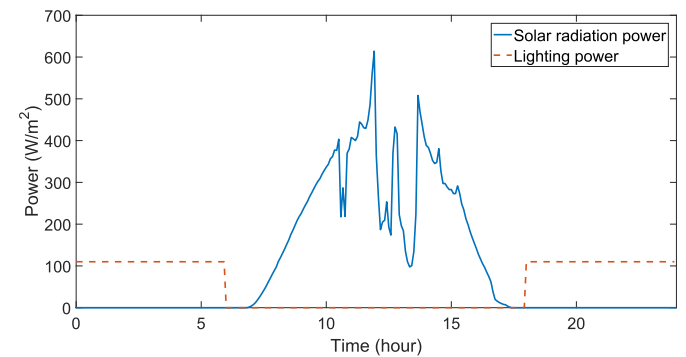**Fig. 4.** Outside temperature and relative humidity.

Fig. 5. Solar irradiation power and lighting power.

meet the system state constraints. The initial values of the temperature, relative humidity, and CO_2 concentration in the greenhouse are set to 20 °C, 74%, and 500 ppm respectively. The

greenhouse climate data sampling interval T_s and the total simulation time T are set to 300 s and 24 h respectively.

Simulations are carried out in MATLAB environment, and the 'fmincon' function is used to solve the optimization problem with the sequential quadratic programming algorithm.

5.2. Optimization results

5.2.1. Strategy 1

The optimization result of Strategy 1 is shown in Fig. 6. It can be seen that almost all the energy consumed is used for greenhouse heating in the morning (from 6 a.m. to 8 a.m.). That is because the outdoor temperature is low during the night, the heat exchange with the outside environment causes the temperature in the greenhouse to gradually drops to the lower limit. The heater must start working to keep the temperature within the required range. The greenhouse ventilation to reduce the humidity in the greenhouse is mainly around noon time (from 10 a.m. to 3 p.m.). The reason is that the outdoor temperature is higher during this period, the ventilation can reduce indoor humidity without causing energy losses.

5.2.2. Strategy 2

The comparison of optimization results between Strategy 1 and Strategy 2 under the TOU tariff is shown in Fig. 7. The comparison of energy consumption between Strategy 1 and Strategy 2 is shown in Fig. 8. The comparison of energy cost between Strategy 1 and Strategy 2 is shown in Fig. 9. It can be seen that Strategy 2 consumes more energy (4502 kWh) than Strategy 1 (3587 kWh). However, the energy cost of Strategy 2 (R 9050) is less than the energy cost of Strategy 1 (R 9942). That is because Strategy 2 consumes less energy (2591 kWh) than Strategy 1 (3112 kWh) during the peak period when the energy price (R 3.1047/kWh) is much higher than that during standard period (R 0.9446/kWh) and off-peak period (R 0.5157/kWh).

5.2.3. Strategy 3

The optimization result of strategy 3 is shown in Fig. 10. The comparison of the energy and CO_2 consumption of three different strategies is shown in Fig. 11. Fig. 12 shows the comparison of the cost of three different strategies. The optimization results show that less CO_2 supply are needed to keep the CO_2 concentration within the required range. The CO_2 consumption of Strategy 3 is reduced by 96.52% (from 27.28 to 0.95 t) compared with Strategy 1 and Strategy 2. The total cost of Strategy 1, Strategy 2 and Strategy 3 are R 39454, R 38540 and R 11018 respectively. Compared with Strategy 1 and Strategy 2, Strategy 3 reduces total costs by 72.07% and 71.41%, respectively.

5.2.4. Optimization analysis

The previous optimization is based on the meteorological data of one typical winter day in Pretoria, South Africa. In order to make the conclusions more convincing, the proposed strategies were also analyzed based on the meteorological data of the other two winter days (June 5, 2016 and August 3, 2016). The meteorological data is shown in Fig. 14 and Fig. 15.

Similar results to the optimization based on the meteorological data of July 13, 2016 are obtained. For June 5, 2016, the operation cost of Strategy 1, Strategy 2 and Strategy 3 are R 41076, R 40576 and R 13317 respectively. Compared with Strategy 1 and Strategy 2, Strategy 3 can reduce operating cost by 67.58% and 67.18% respectively. For August 3, 2016, the operation cost of Strategy 1, Strategy 2 and Strategy 3 are R 37935, R 36687 and R 9966 respectively. Compared with Strategy 1 and Strategy 2, Strategy 3 can reduce operating cost by 73.73% and 72.84% respectively.

5.3. Model predictive control

In (Van Beveren et al., 2015a, b), an open loop control strategy is proposed for greenhouse climate control. Due to the disturbances in the greenhouse system, the accuracy of open loop control is often not high. In this paper, a closed-loop model predictive control strategy is studied and compared with the open loop control strategy.

In this paper, the optimization results of Strategy 3 shown in Fig. 10 are taken as the reference trajectories. The reason for
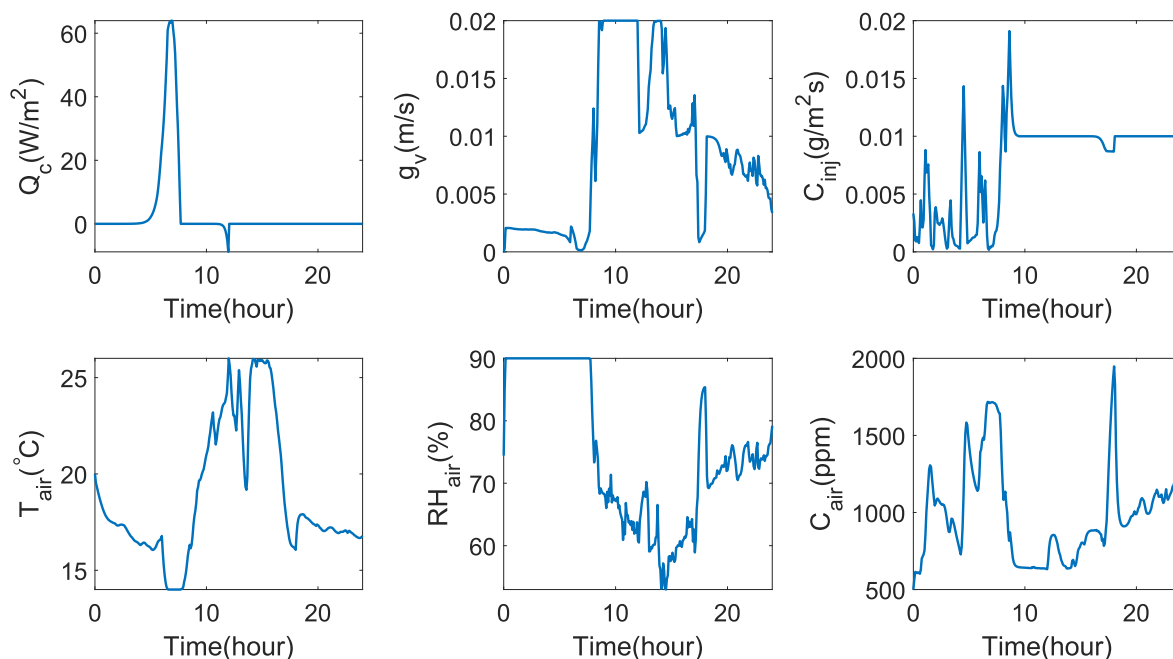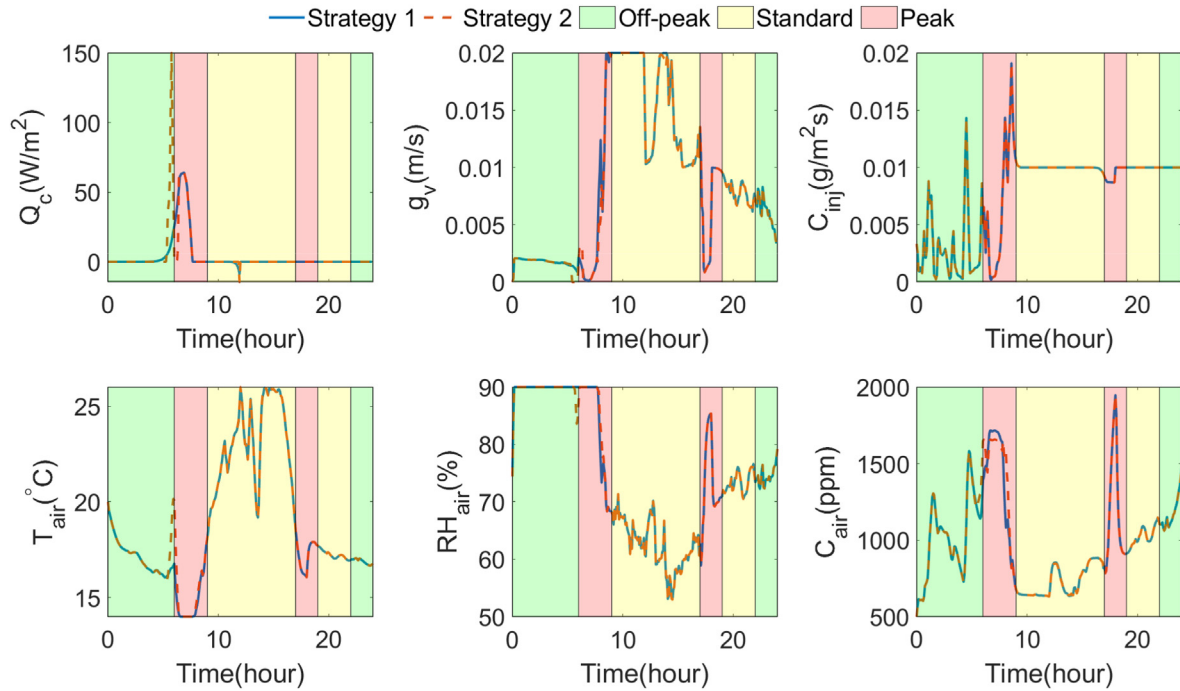

Fig. 6. Optimization results of Strategy 1.

Fig. 7. Comparison of optimization results between Strategy 1 and Strategy 2 under the TOU tariff.
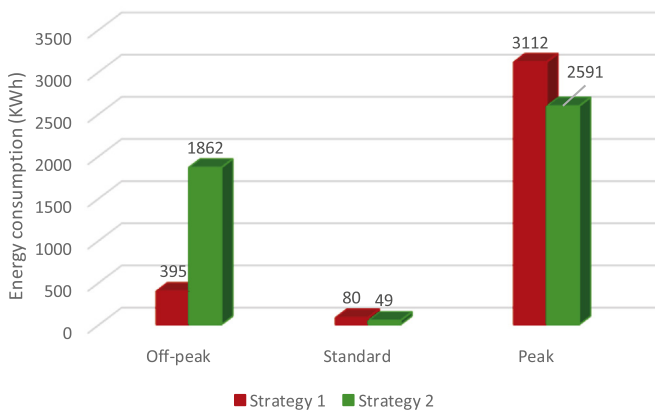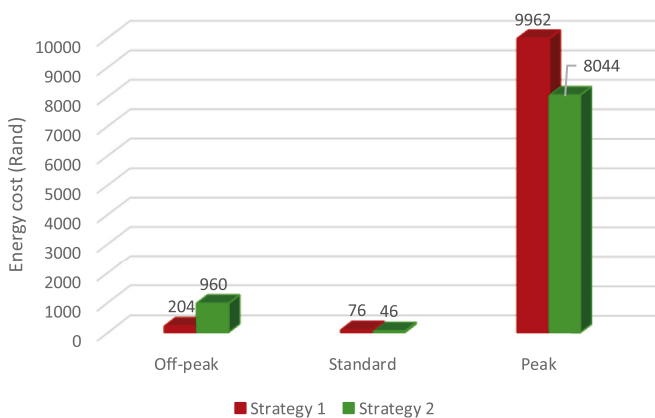

Fig. 8. Energy consumption comparison.

Fig. 9. Energy cost comparison.

choosing the results of Strategy 3 as the reference trajectory is that Strategy 3 is superior to Strategy 2 and Strategy 1 in improving greenhouse energy efficiency and reducing production costs. The operating cost under Strategy 3 is lower than that under Strategy 1 and Strategy 2. The MPC parameter settings are as follows: the predictive horizon $N_p = 10$, the control horizon $N_c = N_p$, the sampling interval $T_s = 60$ s, the total simulation time $T = 24$ h, the weighting matrix $Q = \text{diag}(100, 100, 100)$, $R = \text{diag}(1, 1, 1)$.

Please note that the disturbance is added to the outputs as measurement disturbance. For example, when the system disturbance is 2%, the actual value $y_a = y_p \times (1 + e)$, where y_p is the model predicted value, e is a random variable between -2% and 2%. The comparison results between open loop control and MPC under 2% system disturbances are shown in Fig. 13. It can be seen that three green curves (MPC results) fluctuate in a very small range near the corresponding reference trajectories. However, three red curves (open loop control results) fluctuate in a relatively large range near the corresponding reference trajectories. Compared with open loop control, MPC has better tracking performance.

To compare the tracking performance of open loop control and MPC more accurately, the tracking performance indices relative average deviation (RAD) and maximum relative deviation (MRD) are introduced. The RAD is to evaluate the overall tracking effect while the MRD is to evaluate tracking effect of the worst tracking point.

Denote the value of actual measurement as x_{meas}, then the relative deviation (RD) of x is defined by:

$$\text{RD}(i) = \left| \frac{x_{meas}(i) - x_{ref}(i)}{x_{ref}(i)} \right|. \tag{44}$$

The RAD can be obtained by:
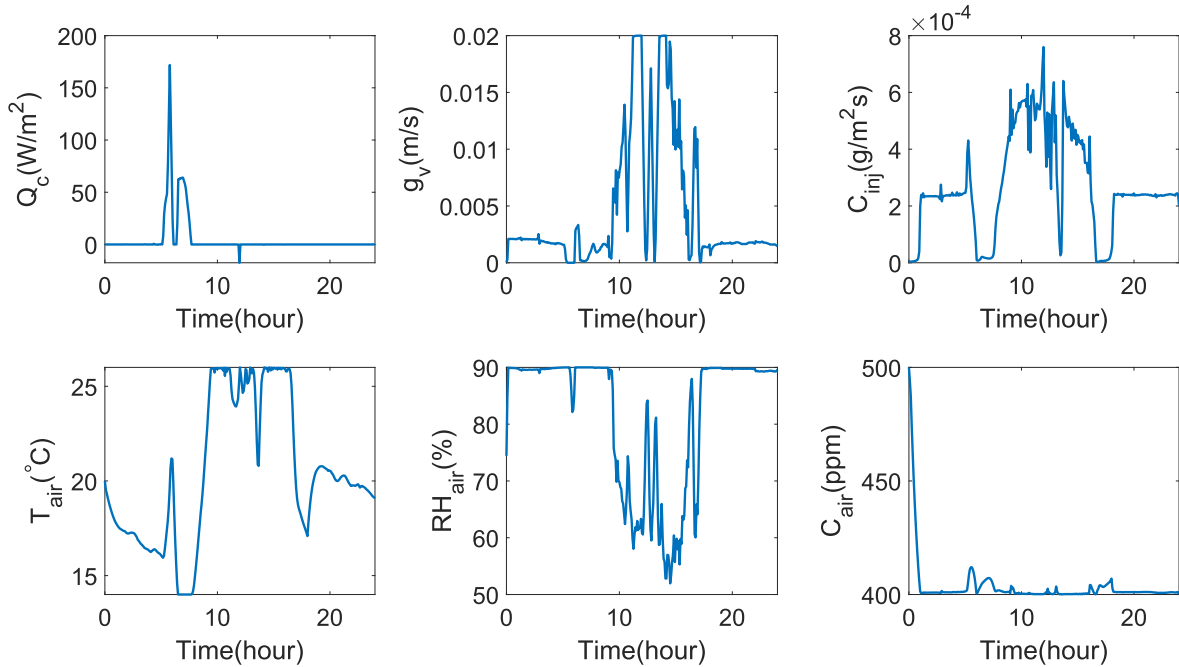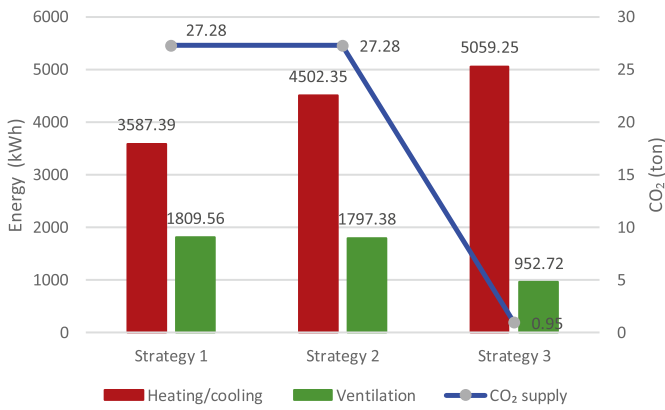
Fig. 10. Optimization results of Strategy 3.

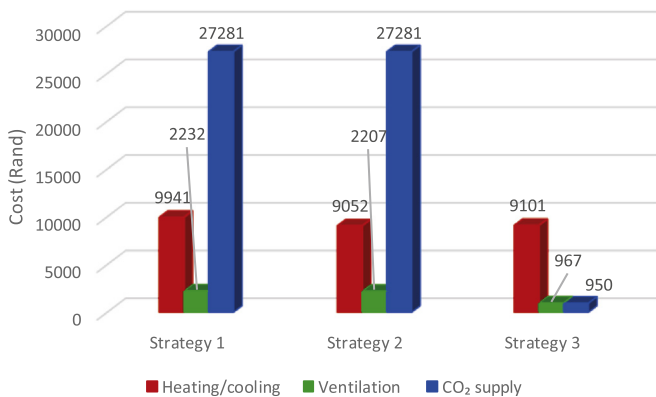**Fig. 11.** Comparison of energy and CO_2 consumption.

Fig. 12. Comparison of the cost of three different strategies.

$$RAD = \frac{1}{N} \sum_{i=1}^{N} RD(i), \tag{45}$$

where N is the total sampling times. For the open loop control, $N = 288$. For the MPC, $N = 1440$.

The MRD can be calculated by:

$$MRD = \max(RD) \tag{46}$$

Table 3 is the tracking performance indices comparison between open loop control and MPC under three different system disturbances. The subscripts 2, 5 and 10 in Table 3 denote the values are the results under 2%, 5% and 10% system disturbance respectively.

When the system disturbance is 2%, compared with open loop control, MPC reduces 60.06% temperature RAD (from 3.38% to 1.35%), 76.19% relative humidity RAD (from 3.36% to 1.07%), and 78.12% CO_2 concentration RAD (from 4.57% to 1.00%). MPC reduces 54.28% temperature MRD (from 13.80% to 6.31%), 66.28% relative humidity MRD (from 18.18% to 6.13%), and 89.31% CO_2 concentration MRD (from 19.27% to 2.06%).

When the system disturbances are 5% and 10%, similar results are obtained. Both the RAD and MRD of MPC are smaller than that of the open loop control. The results show that the MPC has better tracking performance compared with the open loop control under different levels of system disturbances.

6. Conclusion

A hierarchical control strategy of a Venlo-type greenhouse system is proposed to reduce greenhouse cost while keeping greenhouse climatic conditions such as the temperature, humidity and CO_2 concentration within required ranges. The hierarchical control architecture includes two layers. On the upper layer, three different strategies with different optimization objectives are
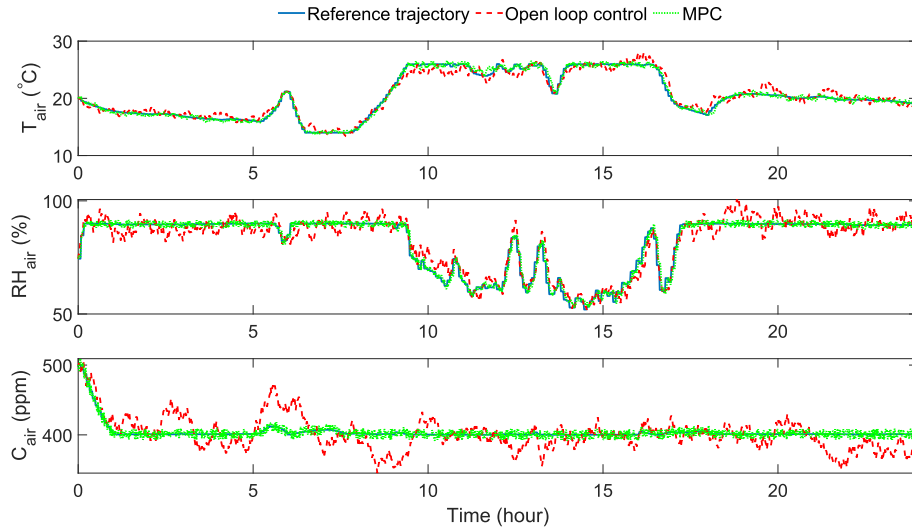
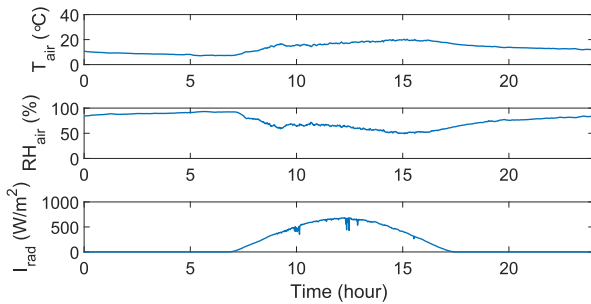**Fig. 13.** Comparison of open loop control and MPC under 2% system disturbances.
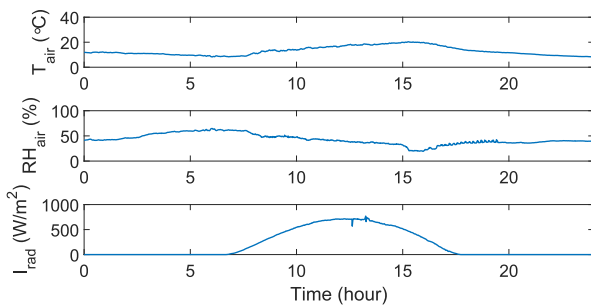

Fig. 14. Meteorological data of June 05, 2016.

Fig. 15. Meteorological data of August 03, 2016.

Table 3
Tracking performance indices comparison between open loop control and MPC under different system disturbances.

	Open loop control		MPC	
	RAD	MRD	RAD	MRD
T_2 (%)	3.38	13.80	1.35	6.31
RH_2 (%)	3.63	18.18	1.07	6.13
C_2 (%)	4.57	19.27	1.00	2.06
T_5 (%)	8.37	37.51	3.23	12.39
RH_5 (%)	8.61	39.62	3.05	29.70
C_5 (%)	11.48	50.40	2.49	6.38
T_{10} (%)	16.62	90.09	7.95	44.96
RH_{10} (%)	17.33	78.77	5.99	80.30
C_{10} (%)	23.07	124.92	4.97	11.15

In future work, we will focus on the following aspects. 1) How to reduce greenhouse water consumption. 2) How to use wind energy, solar energy and other clean energy to power greenhouse systems. 3) How to dispatch hybrid energy systems to operate in a more efficient and clean way.

Declaration of competing interest

The authors declare that they have no known competing financial interests or personal relationships that could have appeared to influence the work reported in this paper.

CRediT authorship contribution statement

Dong Lin: Data curation, Software, Writing - original draft. **Lijun Zhang:** Methodology, Supervision. **Xiaohua Xia:** Writing - review & editing, Supervision.

References

Bennis, N., Duplaix, J., Enéa, G., Haloua, M., Youlal, H., 2008. Greenhouse climate modelling and robust control. Comput. Electron. Agric. 61, 96—107.

Blasco, X., Martínez, M., Herrero, J.M., Ramos, C., Sanchis, J., 2007. Model-based predictive control of greenhouse climate for reducing energy and water consumption. Comput. Electron. Agric. 55, 49—70.

Bontsema, J., Hemming, J., Stanghellini, C., De Visser, P., van Henten, E., Budding, J., Rieswijk, T., Nieboer, S., 2008. On-line estimation of the transpiration in greenhouse horticulture. In: Proceedings Agricontrol 2007. 2nd IFAC International Conference on Modeling and Design of Control Systems in Agriculture, pp. 29—34. Osijek, Croatia.

studied. Strategy 1 is to minimize the energy consumption. Strategy 2 is to minimize the energy cost under the time-of-use (TOU) tariff. Strategy 3 is to minimize the total operating cost. The optimization results are taken as the trajectories for the lower layer. On the lower layer, an MPC controller is designed to track the reference trajectories obtained from the upper layer. Two performance indices are calculated to compare the tracking performance of the proposed MPC controller and an open loop controller under different level of system disturbances. The simulation results show that compared with Strategy 1 and Strategy 2, Strategy 3 reduces total costs by 72.07% and 71.41%, respectively. In addition, the MPC can track the reference trajectories better than the open loop control under three different level system disturbances.

Bozchalui, M.C., Cañizares, C.A., Bhattacharya, K., 2014. Optimal energy management of greenhouses in smart grids. IEEE Trans. Smart Grid 6, 827–835.

Cao, Y., Du, J., Soleymanzadeh, E., 2019. Model predictive control of commercial buildings in demand response programs in the presence of thermal storage. J. Clean. Prod. 218, 315–327.

Chen, J., Xu, F., Tan, D., Shen, Z., Zhang, L., Ai, Q., 2015. A control method for agricultural greenhouses heating based on computational fluid dynamics and energy prediction model. Appl. Energy 141, 106–118.

Chen, J., Yang, J., Zhao, J., Xu, F., Shen, Z., Zhang, L., 2016. Energy demand forecasting of the greenhouses using nonlinear models based on model optimized prediction method. Neurocomputing 174, 1087–1100.

Chen, L., Du, S., Xu, D., He, Y., Liang, M., 2018. Sliding mode control based on disturbance observer for greenhouse climate systems. Math. Probl Eng. 2018, 2071585 https://doi.org/10.1155/2018/2071585.

Coelho, J., de Moura Oliveira, P., Cunha, J.B., 2005. Greenhouse air temperature predictive control using the particle swarm optimisation algorithm. Comput. Electron. Agric. 49, 330–344.

Cuce, E., Harjunowibowo, D., Cuce, P.M., 2016. Renewable and sustainable energy saving strategies for greenhouse systems: a comprehensive review. Renew. Sustain. Energy Rev. 64, 34–59.

Du, J., Bansal, P., Huang, B., 2012. Simulation model of a greenhouse with a heat-pipe heating system. Appl. Energy 93, 268–276.

Durand, H., Ellis, M., Christofides, P.D., 2016. Economic model predictive control designs for input rate-of-change constraint handling and guaranteed economic performance. Comput. Chem. Eng. 92, 18–36.

Erna du Plessis, E., Workneh, T., Laing, M., 2015. Greenhouse cooling systems and models for arid climate. In: Sustainable Agriculture Reviews. Springer, pp. 181–215.

Esen, M., Yuksel, T., 2013. Experimental evaluation of using various renewable energy sources for heating a greenhouse. Energy Build. 65, 340–351.

Ferreira, P.M., Faria, E., Ruano, A., 2002. Neural network models in greenhouse air temperature prediction. Neurocomputing 43, 51–75.

Fox, J.A., Adriaanse, P., Stacey, N.T., 2019. Greenhouse energy management: the thermal interaction of greenhouses with the ground. J. Clean. Prod. 235, 288–296.

Frausto, H.U., Pieters, J.G., 2004. Modelling greenhouse temperature using system identification by means of neural networks. Neurocomputing 56, 423–428.

Garg, N., Dadhich, S.M., 2014. A proposed method to determine yield response factors of different crops under deficit irrigation using inverse formulation approach. Agric. Water Manag. 137, 68–74.

Gruber, J., Guzmán, J., Rodríguez, F., Bordons, C., Berenguel, M., Sánchez, J., 2011. Nonlinear MPC based on a volterra series model for greenhouse temperature control using natural ventilation. Contr. Eng. Pract. 19, 354–366.

Hassanien, R.H.E., Li, M., Lin, W.D., 2016. Advanced applications of solar energy in agricultural greenhouses. Renew. Sustain. Energy Rev. 54, 989–1001.

Hu, H., Xu, L., Wei, R., Zhu, B., 2011. Multi-objective control optimization for greenhouse environment using evolutionary algorithms. Sensors 11, 5792–5807.

Kläring, H.-P., Hauschild, C., Heißner, A., Bar-Yosef, B., 2007. Model-based control of co2 concentration in greenhouses at ambient levels increases cucumber yield. Agric. For. Meteorol. 143, 208–216.

Kohler, M., 2014. Differential electricity pricing and energy efficiency in South Africa. Energy 64, 524–532.

Lafont, F., Balmat, J.-F., 2002. Optimized fuzzy control of a greenhouse. Fuzzy Set Syst. 128, 47–59.

Linker, R., Gutman, P., Seginer, I., 1999. Robust controllers for simultaneous control of temperature and co2 concentration in greenhouses. Contr. Eng. Pract. 7, 851–862.

Liu, X., Guo, P., Li, F., Zheng, W., 2019. Optimization of planning structure in irrigated district considering water footprint under uncertainty. J. Clean. Prod. 210, 1270–1280.

Liu, X., Shi, L., Engel, B.A., Sun, S., Zhao, X., Wu, P., Wang, Y., 2020. New challenges of food security in northwest China: water footprint and virtual water perspective. J. Clean. Prod. 245, 118939.

Mei, J., Xia, X., 2017. Energy-efficient predictive control of indoor thermal comfort and air quality in a direct expansion air conditioning system. Appl. Energy 195, 439–452.

Mei, J., Xia, X., Song, M., 2018. An autonomous hierarchical control for improving indoor comfort and energy efficiency of a direct expansion air conditioning system. Appl. Energy 221, 450–463.

Menyah, K., Wolde-Rufael, Y., 2010. Energy consumption, pollutant emissions and economic growth in South Africa. Energy Econ. 32, 1374–1382.

Mohd, N., Aziz, N., 2016. Performance and robustness evaluation of nonlinear autoregressive with exogenous input model predictive control in controlling industrial fermentation process. J. Clean. Prod. 136, 42–50.

Ramírez-Arias, A., Rodríguez, F., Guzmán, J.L., Berenguel, M., 2012. Multiobjective hierarchical control architecture for greenhouse crop growth. Automatica 48, 490–498.

Rodríguez, F., Guzmán, J., Berenguel, M., Arahal, M., 2008. Adaptive hierarchical control of greenhouse crop production. Int. J. Adapt. Contr. Signal Process. 22, 180–197.

Sayadi, S., Tsatsaronis, G., Morosuk, T., Baranski, M., Sangi, R., Müller, D., 2019. Exergy-based control strategies for the efficient operation of building energy systems. J. Clean. Prod. 241, 118277.

Shen, Y., Wei, R., Xu, L., 2018. Energy consumption prediction of a greenhouse and optimization of daily average temperature. Energies 11, 65.

Su, Y., Xu, L., Li, D., 2015. Adaptive fuzzy control of a class of MIMO nonlinear system with actuator saturation for greenhouse climate control problem. IEEE Trans. Autom. Sci. Eng. 13, 772–788.

Su, Y., Xu, L., Li, D., 2016. Adaptive fuzzy control of a class of mimo nonlinear system with actuator saturation for greenhouse climate control problem. IEEE Trans. Autom. Sci. Eng. 13, 772–788.

Su, Y., Xu, L., Goodman, E.D., 2017. Greenhouse climate fuzzy adaptive control considering energy saving. Int. J. Contr. Autom. Syst. 15, 1936–1948.

Su, Y., Xu, L., Goodman, E.D., 2018. Nearly dynamic programming nn-approximation–based optimal control for greenhouse climate: a simulation study. Optim. Contr. Appl. Methods 39, 638–662.

Tap, F., 2000. Economics-based Optimal Control of Greenhouse Tomato Crop Production. Ph.D. thesis Wageningen Agricultural University, Wageningen, The Netherlands.

Vadiee, A., Martin, V., 2014. Energy management strategies for commercial greenhouses. Appl. Energy 114, 880–888.

Van Beveren, P., Bontsema, J., Van Straten, G., Van Henten, E., 2015a. Minimal heating and cooling in a modern rose greenhouse. Appl. Energy 137, 97–109.

Van Beveren, P., Bontsema, J., Van Straten, G., Van Henten, E., 2015b. Optimal control of greenhouse climate using minimal energy and grower defined bounds. Appl. Energy 159, 509–519.

Van Henten, E., 1994. Greenhouse Climate Management: an Optimal Control Approach. Ph.D. thesis. Wageningen Agricultural University, Wageningen, The Netherlands.

Van Henten, E., Bontsema, J., 2009. Time-scale decomposition of an optimal control problem in greenhouse climate management. Contr. Eng. Pract. 17, 88–96.

Wanjiru, E.M., Zhang, L., Xia, X., 2016. Model predictive control strategy of energy-water management in urban households. Appl. Energy 179, 821–831.

Wu, Z., Tazvinga, H., Xia, X., 2015. Demand side management of photovoltaic-battery hybrid system. Appl. Energy 148, 294–304.

Yang, S.-H., Rhee, J.Y., 2013. Utilization and performance evaluation of a surplus air heat pump system for greenhouse cooling and heating. Appl. Energy 105, 244–251.

Yano, A., Cossu, M., 2019. Energy sustainable greenhouse crop cultivation using photovoltaic technologies. Renew. Sustain. Energy Rev. 109, 116–137.

Zhang, L., Zhuan, X., 2013. Braking-penalized receding horizon control of heavy-haul trains. IEEE Trans. Intell. Transport. Syst. 14, 1620–1628.

Zhang, L., Zhuan, X., 2015. Development of an optimal operation approach in the mpc framework for heavy-haul trains. IEEE Trans. Intell. Transport. Syst. 16, 1391–1400.

Zhu, B., Tazvinga, H., Xia, X., 2014. Switched model predictive control for energy dispatching of a photovoltaic-diesel-battery hybrid power system. IEEE Trans. Contr. Syst. Technol. 23, 1229–1236.